IOPscience iopscience.iop.org

Home Search Collections Journals About Contact us My IOPscience

Study of damage in ion-irradiated α-SiC by optical spectroscopy

This article has been downloaded from IOPscience. Please scroll down to see the full text article.

2006 J. Phys.: Condens. Matter 18 8493

(http://iopscience.iop.org/0953-8984/18/37/008)

View the table of contents for this issue, or go to the journal homepage for more

Download details:
IP Address: 129.252.86.83
The article was downloaded on 28/05/2010 at 13:44

Please note that terms and conditions apply.

INSTITUTE OF PHYSICS PUBLISHING JOURNAL OF PHYSICS: CONDENSED MATTER

J. Phys.: Condens. Matter **18** (2006) 8493–8502 doi:10.1088/0953-8984/18/37/008

Study of damage in ion-irradiated α-SiC by optical spectroscopy

S Sorieul[1], **J-M Costantini**[1,6], **L Gosmain**[2], **G Calas**[3], **J-J Grob**[4] **and L Thomé**[5]

[1] CEA/Saclay, DMN/SRMA, 91191 Gif sur Yvette Cedex, France
[2] CEA/Saclay, DMN/SEMI, 91191 Gif sur Yvette Cedex, France
[3] IMPMC, Laboratoire de Minéralogie-Cristallographie, UMR CNRS 7590, Universités Paris 6 et 7 and IPGP, Case 115, 4 Place Jussieu, 75252 Paris Cedex 05, France
[4] InESS (PHASE), UMR 7163, 23 rue du Loess, BP 20, 67037 Strasbourg Cedex 2, France
[5] CSNSM, CNRS/IN2P3, Université Paris Sud, 91405 Orsay Cedex, France

E-mail: jean-marc.costantini@cea.fr

Received 31 March 2006, in final form 30 June 2006
Published 1 September 2006
Online at stacks.iop.org/JPhysCM/18/8493

Abstract
UV–visible absorption and Raman scattering spectroscopy were used to investigate the effects of 4 MeV Xe-ion and 4 MeV Au-ion irradiations on α-SiC single crystals. The evolution of transmission spectra upon irradiation evidences an increase of the optical absorption. The optical band-gap energy decreases versus fluence, which is linked to band-gap closure attributed to the creation of localized states into the forbidden energy band. A strong effect of the irradiation temperature is observed as a result of dynamic annealing enhanced by the temperature increase. The Urbach energy increases versus fluence due to disorder accumulation in the damaged layer. Comparison of Urbach energy and disorder parameters extracted from Raman spectra shows that the Urbach energy is sensitive to the disorder induced by the accumulation of point defects.

1. Introduction

Silicon carbide (SiC) is widely studied in particular for its potential nuclear applications. In this context, experimental and theoretical efforts have contributed, in the last decades, to the understanding of irradiation-damage processes in SiC essentially at low temperature [1, 2]. Although the wide band gap of SiC allows operation at elevated temperatures, data on the creation of radiation damage at high temperature are still limited and scattered.

The influence of damage accumulation on structural and energetic properties is not easily determined by techniques such as Rutherford backscattering spectroscopy and transmission electron microscopy [3–6]. By contrast, non-destructive spectroscopic methods [7–12] give

[6] Author to whom any correspondence should be addressed.

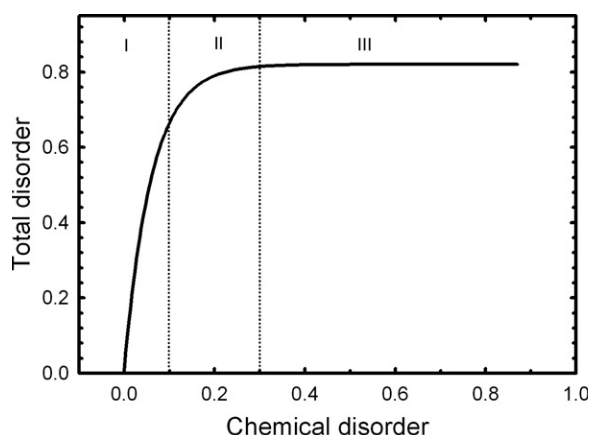

Figure 1. Sketch of the variations of the total disorder versus the chemical disorder induced by irradiation with Au and Xe ions [19]. Definition of the three stages of amorphization according to Zhang *et al* [22]: stage I corresponds to point defect production, stage II is the growth and the coalescence of amorphous domain, stage III is the amorphization.

selective information on defect formation and associated structural transformations, and can detect some aspects of the transformation between the crystalline and amorphous state. UV–visible spectroscopy can be used to follow the damage accumulation and it allows the study of relevant optical properties of SiC. Irradiation induces point defects that increase the absorption and the refractive index of the material. Furthermore the optical band gap decreases as a consequence of defect accumulation [13–18].

Raman spectroscopy data have recently given unique information on the structural transformations operating during the irradiation of α-SiC [19]. For low fluences, the overall sp^3 bond structure and the chemical order may be almost completely conserved. Increasing fluence induces a progressive destruction of α-SiC and the appearance of several new Si–Si, Si–C, and C–C bands. The amorphous state, observed at the highest irradiation fluences, shows a strong randomization of the Si–Si, Si–C and C–C bonds without evidence of sp^3 modes.

A total disorder parameter may be defined by the structure dependence of Raman spectra of SiC. The total disorder parameter corresponds to the integrated area under the α-SiC first-order modes in the irradiated sample normalized to the value (A^{cryst}) in pure α-SiC ($A_{\mathrm{norm}} = A/A^{\mathrm{cryst}}$) [20]. A chemical disorder parameter (χ) is defined by the relative intensity of Si–C and C–C modes taken as an approximation of the concentration of the corresponding bonds [21]. The TO-phonon line at 766 cm^{-1}, which remains in highly damaged samples, and the mode at 1420 cm^{-1} were used to quantify Si–C and C–C bonds, respectively.

Total and chemical disorder parameters are correlated and change as a function of defect concentration. The chemical disorder parameter is a sensitive indicator of each step of the amorphization process proposed by Zhang *et al* [22]. Three stages were thus defined. The first stage ($\chi < 0.1$) corresponds to the formation of isolated defects. In the second stage ($0.1 < \chi < 0.3$), the disordering rate is enhanced and associated to defect-stimulated amorphization that leads to the growth of amorphous nuclei and coalescence of amorphous domains. The third stage ($\chi > 0.3$) is attributed to the amorphization of the irradiated layer and the eventual formation of a continuous amorphous layer (figure 1) [19].

Raman spectroscopic data of α-SiC irradiated at high temperature indicate that increasing the irradiation temperature induces numerous effects on the α-SiC structure and disorder

accumulation. Higher temperatures stabilize a disordered/distorted state and induce a slackening of the disorder production (total and chemical disorders) due to the enhancement of dynamic annealing.

We therefore focused on the irradiation temperature effects on the UV–visible spectroscopy data of single-crystal α-SiC irradiated with heavy ions. We show that the irradiation temperature is an important parameter, as a result of the enhancement of dynamic annealing with increasing temperature. The optical data give access to band-gap and Urbach energies. The Urbach energy increases with the irradiation dose due to a disorder accumulation in the damaged layer, as evaluated from disorder parameters derived from Raman spectroscopy.

2. Experiments

Hexagonal 6H- and 4H-SiC single-crystal wafers (thickness 500 μm) grown by the Lely method were prepared in the LETI Laboratory (CEA Grenoble, France). The normal to the surface was respectively around 3° and 8° off the [00.1] orientation. Samples were doped with nitrogen in the range 10^{18} cm^{-3}. We used both polytypes of α-SiC since it is known that 6H- and 4H-SiC have a similar behaviour upon irradiation.

6H-SiC samples were irradiated with 4 MeV Au ions at room temperature (RT) and at 400 °C at the ARAMIS facility (Orsay). The temperature of 400 °C is a key value because it is well above the critical temperature of amorphization [6] but low enough to expect some radiation damages despite dynamic annealing induced by the increased temperature. 4H-SiC samples were irradiated with 4 MeV Xe ions at 400 °C at the PHASE facility (Strasbourg, France). Similar conditions of irradiation were done in order to check the possible chemical effect of Au ions during irradiation. Fluences were varied from 10^{12} to 10^{16} cm^{-2} and the beam current density was maintained in the range 0.1–2 μA cm^{-2} in order to avoid high dose-rate effects and excessive target heating.

Irradiation parameters were calculated using the SRIM-2003 code. Ion fluences were converted to their equivalent doses of displacements per atom (dpa) based on the SRIM-2003 full-cascade simulations [23], with a specific gravity of 3.21×10^3 kg m^{-3} and the recommended threshold displacement energies of 20 and 35 eV for C and Si sub-lattices, respectively [24, 25].

RT transmission spectra were recorded using a double beam Cary Vary 5G spectrometer in the 200–2000 nm wavelength range. The spectral resolution varied from 1 nm in the UV region to 3.5 nm in the near-infrared region.

3. Results

3.1. Evolution of the absorption spectra upon irradiation

Transmission spectra of un-irradiated SiC are characterized by a dramatic cutoff at about 300 nm, corresponding to the band-gap energy, and a continuous decrease of the transmission in the near-infrared range, due to phonon-assisted absorption. In addition, our sample displays an absorption band around 600 nm, arising from nitrogen-associated defects [26]. The transmission spectra of α-SiC irradiated by Au ions at RT show a dramatic evolution as a function of the irradiation dose (figure 2(a)). Together with a progressive decrease of the transmission, the fundamental absorption edge shifts towards higher wavelengths, as observed for ion-irradiated SiC [15, 18, 26, 27]. The defect-related absorption band in the visible range is progressively hidden by the red shift of the UV cutoff.

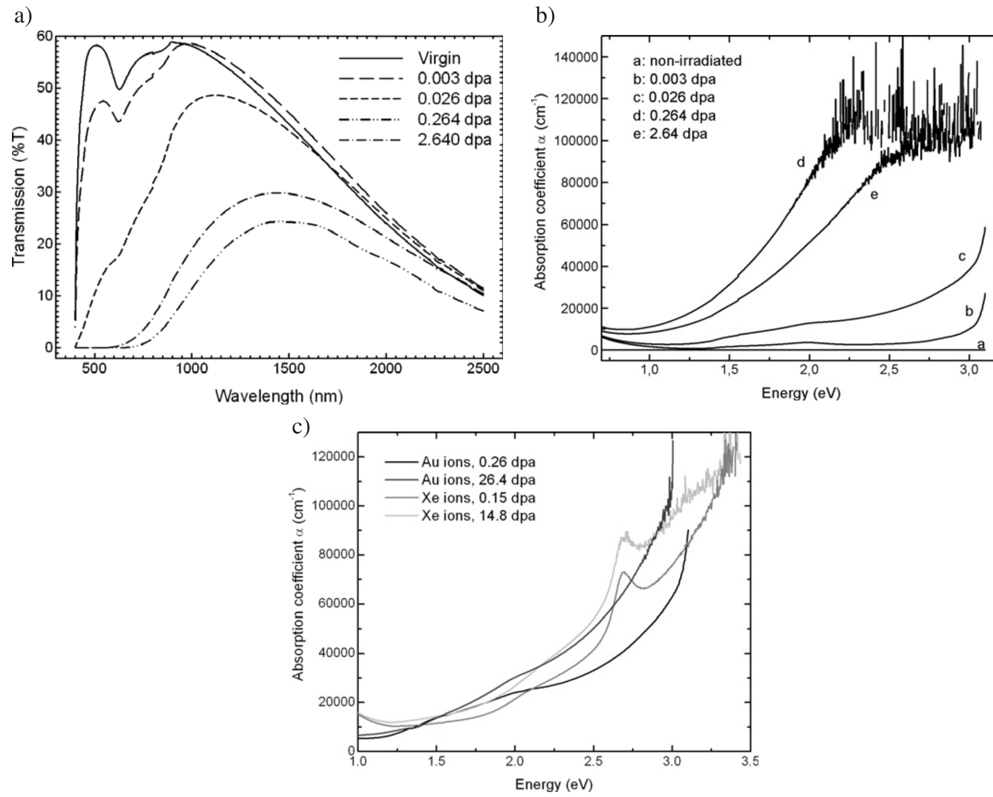

Figure 2. (a) Transmission spectra of Au-ion irradiated 6H-SiC at room temperature for various doses. Absorption coefficient variations versus energy (b) for Au-ion irradiated 6H-SiC at RT (c) for Au- and Xe-ion irradiated 4H-SiC at 400 °C.

The absorption coefficient α is usually derived from an expression based on the Beer–Lambert law:

$$T = \frac{(1-R)^2 \exp[-\alpha d]}{1 - R^2 \exp[-2\alpha d]}, \tag{1}$$

where R is the reflectivity, α is the absorption coefficient, and d is the thickness of the irradiated layer ($d = 0.6$ and 1 μm for Au ions and Xe ions, respectively) [28]. However, equation (1) is only valid in a homogeneous medium. Although the dose is deposited in a heterogeneous way in the sample, we assumed that it can be applied as a first approximation.

Owing to the finite thickness of the damaged layer, another expression based on a two-layer model was also considered [29]:

$$T = (1 - R_i)(1 - R_{iv})(1 - R_v) \exp[-\alpha_v d_v] \exp[-\alpha_i d_i], \tag{2a}$$

with:

$$R = \frac{(n-1)^2}{(n+1)^2}, \tag{2b}$$

where R_i, R_{iv}, R_v are the reflectance of the air/damaged layer, damaged layer/bulk SiC and SiC/air interfaces, α_i and α_v are the absorption coefficient of the damaged and crystalline silicon carbide, d_i and d_v are the thickness of the damaged layer and bulk SiC, and n is the refractive index.

The absorption coefficient α_v is derived from the transmission spectrum of a non-irradiated SiC sample using equation (1). The refractive index n is assumed to be the same ($\approx$2.55) in damaged and undamaged SiC, in agreement with [26]. Therefore, the reflectivity was assumed constant upon irradiation, which implies $R_v = R_i = R$. The reflectivity value deduced from equation (2*b*) is close to 0.2. Furthermore, we assumed that R_{iv} is close to zero, like Musumeci *et al* [29].

The absorption coefficient continuously increases as a function of photon energy, in the visible and near-UV range (figures 2(b) and (c)). Our data confirm that the UV absorption edge of SiC shifts towards lower energies with irradiation, as noticed with other irradiation conditions [14, 18, 26, 30]. The absorption coefficient increases by three orders of magnitude for the highest doses, owing to the accumulation of optically absorbing irradiation-induced centres.

The irradiation temperature has a strong influence on the absorption coefficient, which decreases with increasing temperature (figure 2(c)). This confirms the temperature dependence of the efficiency of radiation-induced defect production in SiC [1, 2]. Optical data demonstrate a simultaneous recovery of defects produced during ion irradiation, due to close-pair recombination and long-range migration of point defects. The difference between data of Xe-ion and Au-ion irradiations are due to the different optical behaviour of both polytypes.

High photon energies give rise to electronic transitions between extended states of the valence and conduction bands. The absorption edge defines the optical band-gap energy E_g. Just above the Tauc region, the energy dependence of the absorption follows an exponential form. This region is defined as the Urbach edge, and is attributed to the electronic transitions from localized states in the band tails to the extended states.

3.2. Optical band gap

The optical absorption coefficient for an indirect gap is given by the Tauc equation (for $\alpha > 10^4\ \mathrm{cm}^{-1}$) [32]:

$$\alpha \times \hbar\omega \propto (\hbar\omega - E_g)^2, \tag{3}$$

where E_g is the optical band-gap energy and $\hbar\omega$ is the photon energy. The value of E_g is obtained graphically by a graphical extrapolation and by a fit of the straight-line portion of the $\sqrt{\alpha \times \hbar\omega} = f(\hbar\omega)$ curve for $3.0 \leqslant \hbar\omega \leqslant 3.2$ eV for 6H-SiC, or $3.0 \leqslant \hbar\omega \leqslant 3.9$ eV for 4H-SiC. Taking α-values derived from equations (1) and (2), the evolution of the optical absorption spectra indicates that the optical band-gap energy decreases as a function of the irradiation dose down to a saturation level (figure 3). In electron- [33] and ion-irradiated SiC [18, 26, 27, 30], similar variations were assigned to the formation of localized levels located near the gap edges and induced by the accumulation of radiation defects. The presence of saturation in samples irradiated at RT has been correlated to the formation of an amorphous buried layer [15, 29].

The band-gap decrease follows an exponential law such as

$$E_g = y_0 + E_g^0 \exp(-\sigma D), \tag{4}$$

where σ is the 'cross-section' of the process (in dpa^{-1}), D is the dose (in dpa), y_0 is a constant and E_g^0 is the saturation value [27]. The cross-section values are 7.93, 0.07 and 7.38 dpa^{-1} for Au-ion irradiation at RT and 400 °C, and Xe-ion irradiation at 400 °C, respectively. As reflected by the cross-section values, the irradiation conditions have a drastic effect on the optical band-gap closure. Increasing the irradiation temperature decreases the cross-section by two orders of magnitude. At the same time, the band-gap closure is more progressive (figure 3), owing to close-pair recombination and thermally assisted long-range migration of point defects. The Xe-ion irradiation at 400 °C show a more limited temperature effect and the cross-section is

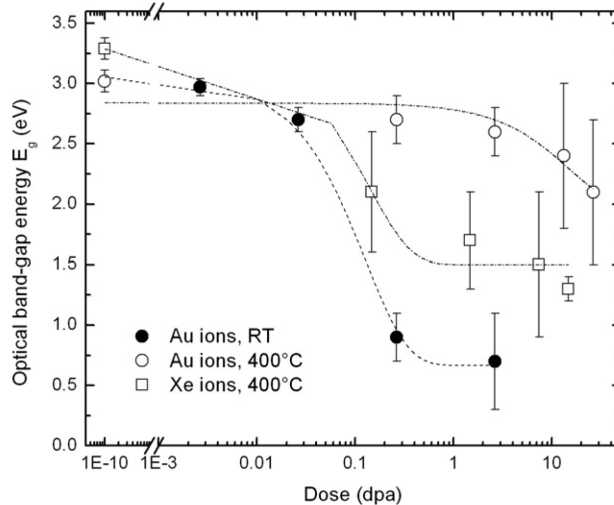

Figure 3. Optical band-gap energy versus dose for 4 MeV Au-ion irradiated 6H-SiC at RT and 400 °C and for 4 MeV Xe-ion irradiated 4H-SiC at 400 °C. Dashed and dash–dotted lines represent least-squares fits to an exponential decay for RT and high-temperature irradiations, respectively.

almost as high as those obtained for RT irradiation. This might come from chemical effects which were not observed by Raman spectroscopy [19].

3.3. Urbach edge

Below the band-gap edge, the sub-gap exponential absorption corresponds to the Urbach edge [31]:

$$\alpha \propto \exp\left(\frac{\hbar\omega}{E_{\mathrm{u}}}\right), \tag{5}$$

where E_{u} is the Urbach energy which accounts for the distribution of the energy of the localized states in the valence band tail for $1.5 \leqslant \hbar\omega \leqslant 3.0$ eV for both polytypes. Urbach edges were already observed for crystalline and amorphous semiconductors like Si [34, 35] and SiC [26]. The E_{u} energy may be determined from the $\ln(\alpha) = f(\hbar\omega)$ curve by a fit of the straight-line part of the curve. Least-squares fits were performed on absorption curves deduced from equations (2) and (3) and the average value was taken as the E_{u} energy.

The Urbach energy increases versus dose following an exponential law and reaches a saturation state at around 0.03 dpa for the RT irradiation (figure 4). The increase of the Urbach energy is in general associated to increasing disorder which creates localized states within the band tails of electronic states, and induces a broadening of Urbach tails [31, 32, 35–37].

The irradiation of SiC by heavy ions at high temperature is characterized by a reduction of defect accumulation with increasing irradiation temperature [39, 38]. The Urbach energy should therefore be lower for irradiations at high temperature than at RT. It is clearly not the case here since the E_{u} energy determined for high-temperature irradiation is at least as large as for RT irradiation. An increase of the irradiation temperature leads to the formation of extended defects as stacking faults, dislocation loops [40, 41], and vacancy clusters [42, 43], which are produced by interstitial migration and aggregation. Because of the accumulation of extended defects, a non-negligible structural disorder is detected by Raman spectroscopy [19].

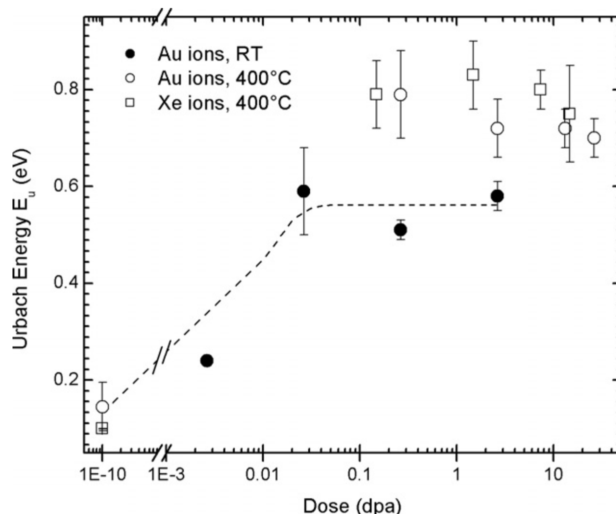

Figure 4. Urbach energy for 4 MeV Au-ion irradiated 6H-SiC at RT and at 400 °C, and for 4 MeV Xe-ion irradiated 4H-SiC at 400 °C. Dashed line represents least-squares fit to an exponential growth for the RT irradiation.

This induced disorder may be the origin of the high Urbach energy value. Similar high values of the E_u energy are obtained for Xe irradiation (figure 4).

4. Discussion

4.1. Extinction and absorption coefficients

Some authors claimed [44] that there is a discrepancy between the absorption coefficient derived from UV–visible absorption spectroscopy and that extracted from the depth profiling of the first-order Raman line intensity using a confocal microprobe setup at 514.5 nm. They attributed this discrepancy to damage effects. However, it is not possible to compare the optical absorption coefficients extracted from Raman spectra with those derived from the Beer–Lambert law, because the two coefficients arise from different optical processes. The value deduced from our Raman spectra [19] corresponds to the extinction coefficient κ, defined as the sum of the absorption coefficient α and the scattering coefficient σ (i.e. $\kappa = \alpha + \sigma$). In order to determine the extinction coefficient κ, the average intensity of the first-order Raman lines (767, 788, 796 and 966 cm^{-1} for 6H; 777, 797 and 967 cm^{-1} for 4H) was plotted with z scan depth. The coefficient κ was extracted from the decreasing part of the intensity curves taking into account the value of the extinction coefficient of the virgin part of the sample. The expression was the following:

$$I = I_0 e^{-\kappa z}. \tag{6}$$

The coefficient κ increases with the absorption coefficient α up to a saturation step (figure 5). The direct correlation between the two optical coefficients confirms the assumption of a decrease of the Raman intensity due to the enhancement of absorption processes by irradiation [1, 45]. The correlation seems to be independent of the irradiation temperature. Xe-ion irradiation gives rise to a different evolution of the optical coefficients. This different behaviour may be attributed to chemical effects.

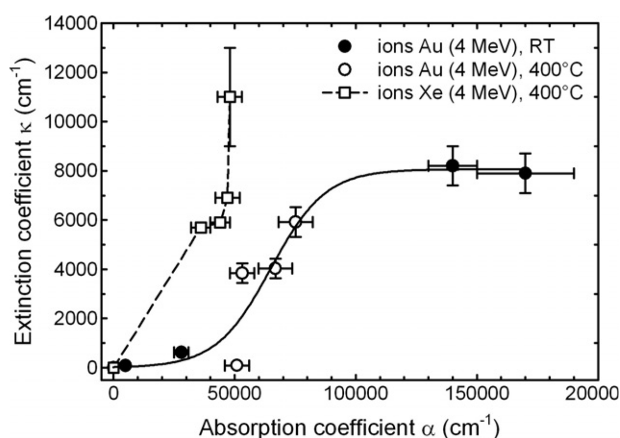

Figure 5. Extinction coefficient κ as a function of the absorption coefficient α for Au-ion irradiated 6H-SiC at room temperature and at 400 °C and Xe-ion irradiated 4H-SiC at 400 °C. The straight line corresponds to a least-squares fit to a sigmoid curve. The dashed line is used as a guide for the eyes.

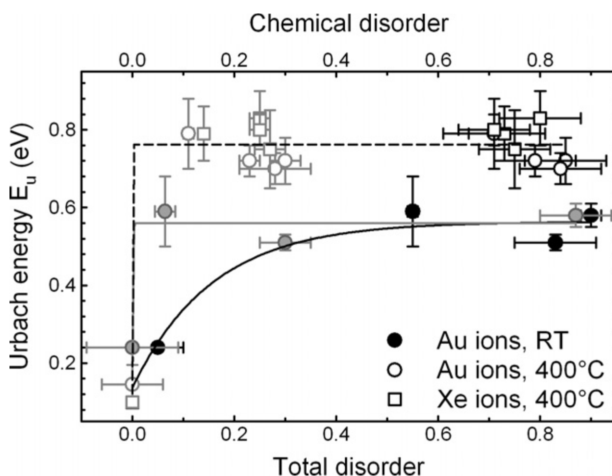

Figure 6. Urbach energy versus total disorder (in black) and chemical disorder (in grey). Both disorder parameters were deduced from Raman spectra for Au-ion irradiated 6H-SiC at room temperature and at 400 °C and Xe-ion irradiated 4H-SiC at 400 °C. Straight lines represent least-squares fits to an exponential growth. The dashed line is used as a guide for the eyes.

4.2. Use of the Urbach energy as a disorder indicator

Rutherford backscattering spectroscopy (RBS/C) is generally used for the study of disorder in silicon carbide [22, 46, 47]. More recently, Raman spectroscopy was also proposed as a good tool for the study of disorder accumulation in irradiated SiC [19, 20]. Figure 6 represents the variations of the Urbach energy as a function of the operational parameters derived from the Raman spectra, total disorder parameter and chemical disorder parameter, (black and grey symbols, respectively). For RT irradiation, the Urbach energy increases versus both total disorder and chemical disorder (figure 6). However, E_u saturates instantaneously as chemical disorder appears after Au-ion irradiation at RT and 400 °C. The corresponding

Raman spectra show that the saturation is reached for a for chemical disorder parameter larger than 0.1 (i.e. when homonuclear bonds are formed). The three stages of the amorphization process presented on figure 1 were observed for Au- and Xe-ion irradiated samples.

The Urbach energy increases only during stage I of amorphization (figure 1) and then saturates. This suggests that the Urbach energy corresponds to disorder produced by the accumulation of radiation point defects. Through analyses of Urbach edges, information on the accumulation of disorder induced by radiation defects can be obtained whereas it cannot be reached by Raman spectroscopy.

5. Conclusions

UV–visible absorption and Raman scattering spectroscopy were used to investigate the effects of heavy-ion irradiations on α-SiC single crystals. The evolution of transmission spectra upon irradiation evidences an increase of the optical absorption and a shift of the fundamental absorption edge to larger wavelengths. Analysis of optical absorption curves allows the determination of the optical band-gap E_g and Urbach E_u energies. The optical band-gap energy decreases versus dose, which is linked to a band-gap closure. This closure is attributed to the creation of localized states into the forbidden energy band. A strong effect of the irradiation temperature was observed as a result of dynamic annealing enhanced by the temperature increase. The Urbach energy increases versus dose due to a disorder accumulation in the damaged layer. The comparison of Urbach energy and disorder parameters extracted from Raman spectra showed that the Urbach energy is sensitive to the disorder induced by the point defect accumulation, which corresponds to the first step of the amorphization process. Besides, the Urbach energy saturates whatever the irradiation conditions.

Acknowledgment

This work was supported by the joint research program ISMIR between CEA and CNRS.

References

[1] Weber W J, Wang L M, Yu N and Hess N J 1998 *Mater. Sci. Eng.* A **253** 62
[2] Wendler E, Heft A and Wesch W 1998 *Nucl. Instrum. Methods Phys. Res.* B **141** 105
[3] Heera V, Prokert F, Schell N, Seifarth H, Fukarek W, Voelskow M and Skorupa W 1997 *Appl. Phys. Lett.* **70** 3531
[4] Jiang W, Weber W J, Thevuthasan S and McCready D E 1999 *Surf. Interface Anal.* **27** 179
[5] Ohno T, Onose H, Sugawara Y, Asano K, Hayashi T and Yatsuo T 1999 *J. Electron. Mater.* **28** 180
[6] Jiang W, Weber W J, Zhang Y, Thevuthasan S and Sutthanandan V 2003 *Nucl. Instrum. Methods Phys. Res.* B **207** 92
[7] Bolse W, Conrad J, Rödle T and Weber T 1995 *Surf. Coat. Technol.* **74/75** 927
[8] Musumeci P, Calcagno L, Grimaldi M G and Foti G 1996 *Appl. Phys. Lett.* **69** 468
[9] Bolse W, Conrad J, Harbsmeier F, Borowski M and Rödle T 1997 *Mater. Sci. Forum* **248/249** 319
[10] Musumeci P, Reitano R, Calcagno L, Roccaforte F, Makhtari A and Grimaldi M G 1997 *Phil. Mag.* B **76** 323
[11] Bolse W 1998 *Nucl. Instrum. Methods Phys. Res.* B **141** 133
[12] Wendler E and Peiter G 2000 *J. Appl. Phys.* **87** 7679
[13] Calcagno L, Grimaldi M G and Musumeci P 1997 *J. Mater. Res.* **12** 1727
[14] Derst G, Wilbertz C, Bhatia K L, Krätschmer W and Kalbitzer S 1989 *Appl. Phys. Lett.* **54** 1722
[15] Musumeci P, Calcagno L, Grimaldi M G and Foti G 1996 *Nucl. Instrum. Methods Phys. Res.* B **116** 327
[16] Musumeci P, Reitano R, Calcagno L, Roccaforte F, Makhtari A and Grimaldi M G 1997 *Phil. Mag.* B **76** 323
[17] Wendler E, Heft A, Wesch W, Peiter G and Dunken H H 1997 *Nucl. Instrum. Methods Phys. Res.* B **127/128** 341
[18] Wendler E and Peiter G 2000 *J. Appl. Phys.* **87** 7679
[19] Sorieul S, Costantini J-M, Gosmain L, Thomé L and Grob J-J 2006 *J. Phys.: Condens. Matter* **18** 5235

[20] Menzel R, Gärtner K, Wesch W and Hobert H 2000 *J. Appl. Phys.* **88** 5658
[21] Yuan X and Hobbs L W 2002 *Nucl. Instrum. Methods Phys. Res.* B **191** 74
[22] Zhang Y, Weber W J, Jiang W, Wang C M and Shutthanandan V 2004 *J. Appl. Phys.* **95** 4012
[23] Ziegler F, Biersack J P and Littmarck U 1985 *The Stopping and Range of Ions in Solids* (New York: Pergamon)
[24] Devanathan R and Weber W J 2000 *J. Nucl. Mater.* **278** 258
[25] Lucas G and Pizzagalli L 2005 *Nucl. Instrum. Methods Phys. Res.* B **229** 359
[26] Wendler E, Heft A, Zammit U, Glaser E, Marinelli M and Wesch W 1996 *Nucl. Instrum. Methods Phys. Res.* B **116** 398
[27] Compagnini G, Foti G, Reitano R and Mondio G 1993 *J. Non-Cryst. Solids* **162** 237
[28] Pankove J I 1971 *Optical Processes in Semiconductors* (Englewood Cliffs, NJ: Prentice-Hall)
[29] Musumeci P, Calcagno L, Grimaldi M G and Foti G 1996 *Appl. Phys. Lett.* **69** 468
[30] Levalois M, Lhermitte-Sebire I, Marie P, Paumier E and Vicens J 1996 *Nucl. Instrum. Methods Phys. Res.* B **107** 239
[31] Mott N F and Davis E A 1979 *Electronic Processes in Non-Crystalline Materials* 2nd edn (Oxford: Clarendon)
[32] Tauc J 1974 *Amorphous and Liquid Semiconductors* ed J Tauc (London: Plenum) pp 170–95
[33] Yasuda K, Takeda M, Masuda H and Yoshida A 1982 *Phys. Status Solidi* a **71** 549
[34] Zammit U, Gasparrini F, Marinelli M, Pizzoferrato R, Agostini A and Mercuri F 1991 *J. Appl. Phys.* **70** 7060
[35] Tripura Sundari S 2004 *Nucl. Instrum. Methods Phys. Res.* B **215** 157
[36] Rincon C, Wasim S M, Marin G, Marquez R, Nieves L, Sanchez Perez G and Medina E 2001 *J. Appl. Phys.* **90** 4423
[37] Rusli K, Yoon S F, Ahn J, Ligatchev V, Teo E J, Osipowicz T and Watt F 2002 *J. Appl. Phys.* **92** 2937
[38] Jiang W, Weber W J, Zhang Y, Thevuthasan S and Sutthanandan V 2003 *Nucl. Instrum. Methods Phys. Res.* B **207** 92
[39] Jiang W, Zhang Y and Weber W J 2004 *Phys. Rev.* B **70** 165208
[40] Ohno T, Onose H, Sugawara Y, Asano K, Hayashi T and Yatsuo T 1999 *J. Electron. Mater.* **28** 180
[41] Ishimaru M, Dickerson R M and Sickafus K E 1999 *Appl. Phys. Lett.* **75** 352
[42] Itoh H, Uedono A, Ohshima T, Aoki Y, Yoshikawa M, Nashiyama I, Tanigawa S, Okumura H and Sadafumi Y 1997 *Appl. Phys.* A **65** 315
[43] Slotte J, Saarinen K, Janson M S, Hallén A, Kuznetsov A Yu, Svensson B G, Wong-Leung J and Jagadish C 2005 *J. Appl. Phys.* **97** 033513
[44] Campos F J, Mestres N, Morvan E, Godignon P and Millan J 1999 *J. Appl. Phys.* **85** 99
[45] Héliou R, Brebner J L and Roorda S 2001 *Nucl. Instrum. Methods Phys. Res.* B **175–177** 268
[46] Jiang W and Weber W J 2001 *Phys. Rev.* B **64** 125206
[47] Weber W J, Jiang W and Thevuthasan S 2001 *Nucl. Instrum. Methods Phys. Res.* B **175–177** 26